Short Communication

Preparation and Corrosion Behavior of Chemically Bonded Ceramic Coatings Reinforced by Functionalized Graphene Oxide

Yongxin Guo[1], Da Bian[1,2,], Guoqiang Jiang[1], Yongwu Zhao[1,2]**

[1] College of Mechanical Engineering, Jiangnan University, Wuxi 214100, Jiangsu, China
[2] Jiangsu Key Laboratory of Advanced Food Manufacturing Equipment and Technology, Jiangnan University, Wuxi 214100, Jiangsu, China
*E-mail: biand@jiangnan.edu.cn ; Zhaoyw@jiangnan.edu.cn

Graphene oxide (GO) was decorated by 3-aminopropyltriethoxysilane (APTES) through the reactions of carboxylic and epoxide groups with amino groups. Then, the chemically bonded ceramic coatings were prepared with the addition of functionalized GO. The dispersion quality of GO in the ceramic matrix was examined by scanning electron microscopy (SEM), which revealed no cracks or space between GO and ceramic matrix. The corrosion protection of the ceramic coatings was characterized by potentiodynamic polarization testing after immersion in 3.5 wt% NaCl solution for 10 h at room temperature. The corrosion resistance of the ceramic coatings was remarkably improved with the addition of the functionalized GO. The protection efficiency of the ceramic coatings increased to 90% with the addition of 0.6 wt% functionalized GO. The enhancement of the anticorrosion performance was mainly attributed to the barrier properties of the well-dispersed functionalized GO in the ceramic matrix.

1. INTRODUCTION

Ceramic coatings have been utilized to protect metallic substrates against corrosion by acting as physical barriers in many areas, including aerospace industry, military and energy industry[1-3]. Many studies have been performed to improve the anticorrosion performance of coatings through the addition of various fillers[4-7].

Graphene oxide (GO), a two dimensional atomic thin layer comprising a carbon network with a very large surface area, can improve the corrosion protection performance of ceramic coatings due to its impermeability to corrosive agents, such as O_2 and H_2O[8-11]. However, the application of GO has been

severely restricted by its poor dispersion in the coating matrix as a filler material due to van der Waals interactions[12-14]. In a previous work[15], a plasma electrolytic oxidation coating was prepared on a AZ31 magnesium alloy reinforced with GO. The results revealed that GO could remarkably improve the corrosion resistance of the coatings. However, increased concentrations of GO decreased the corrosion resistance because of an increased number of micropores and a decrease in the uniformity of the coating. In other studies, the corrosion protection performance of various polymeric materials (such as polyurethane, polyisocyanate, and epoxy resins) reinforced by covalently grafted graphene oxide nanosheets was documented, and the inhomogeneous distribution of the GO in the coating matrix was considered to be one of the most important parameters influencing the coating efficiency/performance of the material[16],[17].

Therefore, the modification of GO consequently becomes a crucial aspect of utilizing them as a filler material in coatings and still requires significant attention from the research community. In this research, GO was functionalized by 3-aminopropyltriethoxysilane (APTES) and added into ceramic coatings to form a chemically bonded composite material. The effect of the functionalized GO on the corrosion protection performance of ceramic coatings was investigated by electrochemical corrosion measurements. In addition, the corrosion resistance mechanism of the ceramic coatings with functionalized GO was also investigated.

2. EXPERIMENTAL

2.1. Raw materials

The ceramic coatings were prepared on AISI 304L stainless steel with a chemical composition (wt. %) of 18.4 Cr, 8.04 Ni, 1.28 Mn, 0.33 Si, 0.052 N, 0.034 P, 0.033 C, and 0.002 S. The substrate with dimensions of 30 mm×30 mm×2 mm was polished with silicon carbide abrasive paper. Then, the substrate was washed with anhydrous ethanol and acetone. Graphene oxide (GO) was provided by Nanjing XFNANO Materials Tech Co., Ltd. The aluminium dihydrogen phosphate ($Al(H_2PO_4)_3$, AP) binder was purchased from Xinxiang Materials Tech Co., Ltd., China. The following materials were purchased from Sinopharm Chemical Reagent Co., Ltd., China: alumina (3.5 µm), zirconia, N, N-dimethylformamide (DMF), 3-aminopropyltriethoxysilane (APTES), anhydrous ethanol, and zinc oxide.

2.2. Chemical functionalization of GO

The coupling agent solution contained 20 wt% APTES, 72 wt% anhydrous ethanol, and 8 wt% deionized water. The mixture was stirred for 1 h to allow the hydrolysis process to occur. Then, GO was dispersed in the DMF and sonicated for 1 h to form a homogeneous suspension. A fixed amount of silane precursor was added into the prepared GO suspension via ultrasonication for 0.5 h. The obtained mixture was stirred at 80 °C for 6 h, and the product was filtered, washed with anhydrous ethanol and DI water several times, and dried in a vacuum oven at 70 °C for 24 h to obtain amino-silane functionalized GO.

2.3 Preparation of the ceramic coatings

The chemically bonded ceramic coatings were prepared on the substrate by brushing it with a mixture of alumina, zinc oxide, zirconia, AP binder and functionalized GO. The powder composites were mixed well with AP binder to form a slurry. Subsequently, the slurry was uniformly coated on the substrate using a brush. All samples were dried at room temperature for 6 h and then cured at the following conditions: 50 °C (1 h), 100 °C (2 h), 150 °C (1 h), 200 °C (1 h) and 280 °C (1 h). The compositions of the chemically bonded ceramic coatings are shown in Table 1.

Table 1. Compositions of chemically bonded ceramic coatings.

Sample (wt%)	alumina	Zinc oxide	Zirconia	AP binder	Functionalized GO
I	44	7	4	45	0
II	43.8	7	4	45	0.2
III	43.6	7	4	45	0.4
IV	43.4	7	4	45	0.6

2.4 Characterization

The morphology of the functionalized GO was observed by SEM (ZEISS EVO18, Germany). The surface morphologies of the ceramic coatings and the dispersion quality of functionalized GO in the coating matrix were observed by scanning electron microscopy (Hitachi SU1510, Japan). The potentiodynamic polarization was carried out by the electrochemistry workstation CHI66C (Shanghai Chenhua instrument Co., LTD, China). All samples were immersed in 3.5 wt% NaCl solution for 10 h prior to measurements. In the test, the coated steel acted as the working electrode with an area of 10 mm×10 mm, the platinum electrode acted as the counter electrode and the saturated calomel electrode (SCE) acted as the reference electrode. The scan rate for the polarization was 2 mV/s, and each sample was measured three times to ensure the measurement repeatability.

3. RESULTS AND DISCUSSION

3.1 Characterization of the functionalized GO

Fig. 1 shows an SEM image of functionalized GO, which exhibits a rough surface with characteristic wavy wrinkles. This confirms that the structure of GO was not destroyed during the decorating process[18]. The thin sheets with puffy structures after functionalization indicate that APTES prevents the agglomeration of GO after decoration. The special structure of functionalized GO is favourable for achieving a homogeneous distribution within the ceramic matrix.
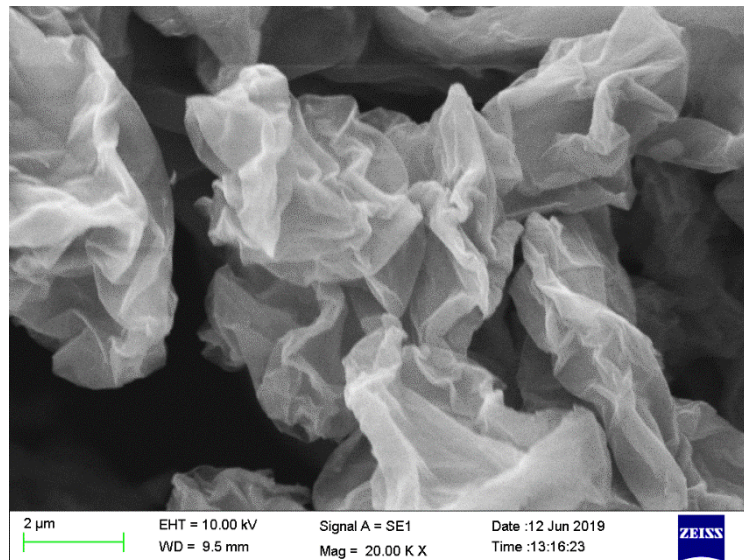
Figure 1. SEM image of functionalized GO.

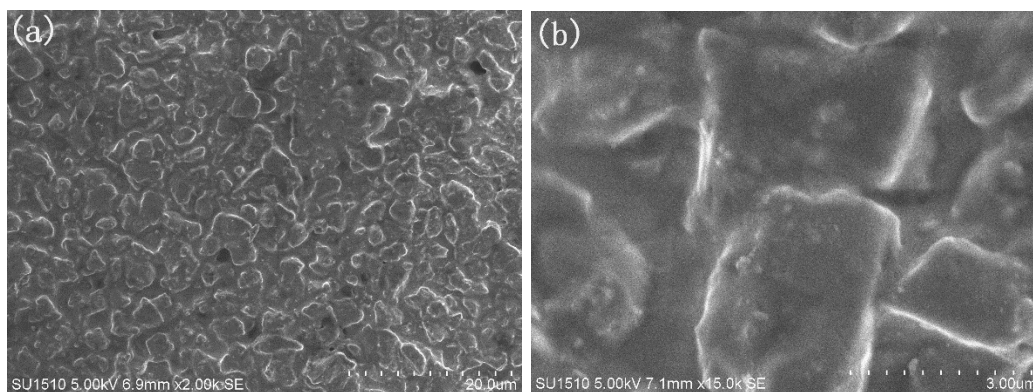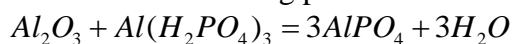*3.2 Characterization of ceramic coatings*

Figure 2. SEM images of the surface of the ceramic coatings at (a) a low magnification of 2.0 kX and (b) a high magnification of 15.0 kX.

As shown in Fig. 2a, no microcrack could be found on the surface of ceramic coatings after curing. The particles are connected well with the binding phase formed during the curing process. The main reactions for the binding phase are as follows[19]:

$$Al_2O_3 + Al(H_2PO_4)_3 = 3AlPO_4 + 3H_2O$$

The product of $AlPO_4$ (berlinite) is a bonding phase that binds individual particles and forms ceramic coatings. As shown in Fig. 2b, at the high magnification image of the coating surface, the particles are almost fully covered by the binding phase. Similar reactions occurred when the samples were cured in the presence of ZnO and ZrO_2 separately[20].
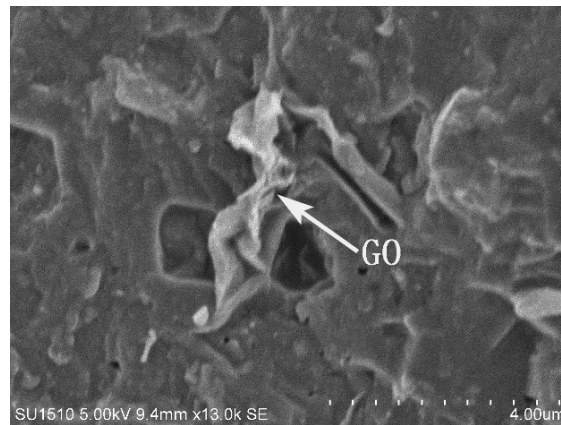
Figure 3. SEM image of the fracture surface of the ceramic coating with functionalized GO.

To investigate the dispersion quality and interfacial interactions of the functionalized GO in a ceramic coating matrix, the fracture surface of ceramic coatings with functionalized GO on the substrate was obtained and is shown in Fig. 3. This reveals that GO is well dispersed in the ceramic coatings and has a thin layer structure. In addition, there is no space between GO and the ceramic coating matrix, which means that the bonding strength between GO and the coating matrix is improved. These results are completely different from the results reported by a previous work[21]. This approach is beneficial for enhancing the anticorrosion performance of ceramic coatings, which was validated by additional measurements.

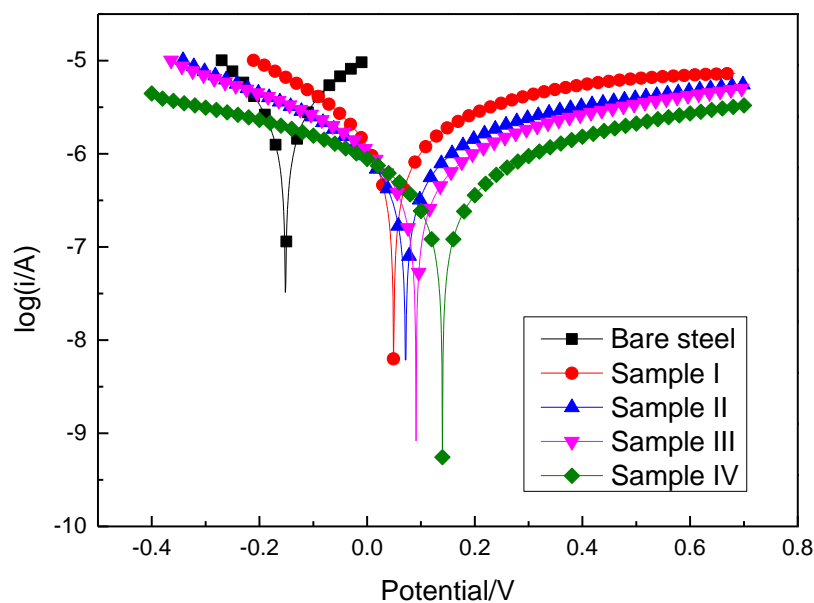*3.3 The corrosion resistance of the ceramic coatings*

Figure 4. Potentiodynamic polarization curves of the bare steel and samples I-IV immersed in the 3.5 wt% NaCl solution.

Table 2. Polarization parameters of the bare steel and samples I-IV.

Samples	Electrochemical parameters		PE (%)
	E_{corr} (V)	I_{corr} (A/cm^2)	
Bare steel	-0.152	2.696e-006	-
Sample I	0.049	0.919e-007	66
Sample II	0.071	5.380e-007	80
Sample III	0.091	4.544e-007	83
Sample IV	0.140	2.647e-007	90

Fig. 4 shows the potentiodynamic polarization curves of the bare steel and ceramic coatings with different contents of functionalized GO. All samples were immersed in 3.5 wt% NaCl aqueous solutions for 10 h before the test. The corrosion potential (E_{corr}) and corrosion current density (i_{corr}) calculated from the polarization curves by Tafel extrapolation are listed in Table 2. The protection efficiency (PE) of the ceramic coatings was calculated according to the following equation:

$$PE \ (\%) = \frac{i_{coor,b} - i_{coor,i}}{i_{coor,b}} \times 100\%$$

where $i_{coor,b}$ and $i_{coor,i}$ are the corrosion current densities of bare steel and coated substrate, respectively.

For the bare steel, the E_{corr} is -0.152 V with the highest corrosion current density of 2.696e-006 (A/cm^2). It is known that E_{corr} mainly represents the tendency for a corrosion reaction, and a low E_{corr} corresponds to a high corrosion rate of the sample[22]. Compared with the bare steel substrate, sample I has a higher corrosion potential (0.049 V) and a lower corrosion current density (0.919 e-007 A/cm^2), indicating that the chemically bonded ceramic coating reduces the corrosion rate of the substrate effectively. Due to the addition of the functionalized GO, the corrosion current density dramatically decreases to 5.380 e-007 A/cm^2 with a corrosion potential of 0.071V. With a gradual increase in the functionalized GO, the value of the E_{corr} and PE of the ceramic coatings increases to 0.140 V and 90%, respectively, with the addition of 0.6 wt% GO. In addition, the value of i_{corr} decreases to 2.647e-007 A/cm^2, indicating that the well-dispersed GO increases the corrosion protection of the ceramic coatings.

The dispersion of GO in the ceramic matrix is improved by decorating it with APTES because it can reduce the cracks and pores caused by the agglomeration of GO. In addition, there are no pores or spaces between the GO and the ceramic matrix, as shown in Fig. 3. Therefore, the ceramic coatings become compact with few cracks and pores inside the ceramic matrix. Thus, with a barrier present, the corrosive electrolyte cannot access the substrate without the presence of cracks and pores. In the case of the non-functionalized sample, H_2O, O_2 and Cl$^-$ can go through the ceramic coatings and access the substrate through cracks in the coating, which leads to corrosion of the substrate. The addition of GO can make the pathway more tortuous because the cracks cannot pass through GO because of its high tensile strength, and the cracks change their direction and pass along the gap between the GO and the ceramic matrix. As shown in Fig. 3, there is no obvious space between the functionalized GO and the ceramic matrix in the present paper. When the cracks reach the GO, they cannot pass through it, so the cracks need to change their direction. Cracks pass through places with the weakest bonding strength.

Obviously, the bonding strength between the functionalized GO and the ceramic matrix is the weakest in this system. Thus, the cracks damage the bonding between the GO and ceramic matrix and propagate along this interface. Therefore, the addition of GO can not only make the cracks more tortuous but also prevent the possibility of cracking by decreasing the fracture energy; this is because damaging the bonding and separating GO and ceramic matrix consumes a large amount of fracture energy. The anticorrosion mechanisms of the ceramic coatings with functionalized GO are shown in Fig. 5. As shown in Fig. 5, the diffusion pathway is blocked because damaging the bonding between the GO and ceramic matrix consumes a substantial amount of fracture energy, and there is not enough energy to develop cracks. Additionally, if there is enough energy to develop cracks, the pathway for the corrosive electrolytes also becomes more tortuous, and it becomes more difficult to access the substrate with functionalized GO because of the need to change direction.
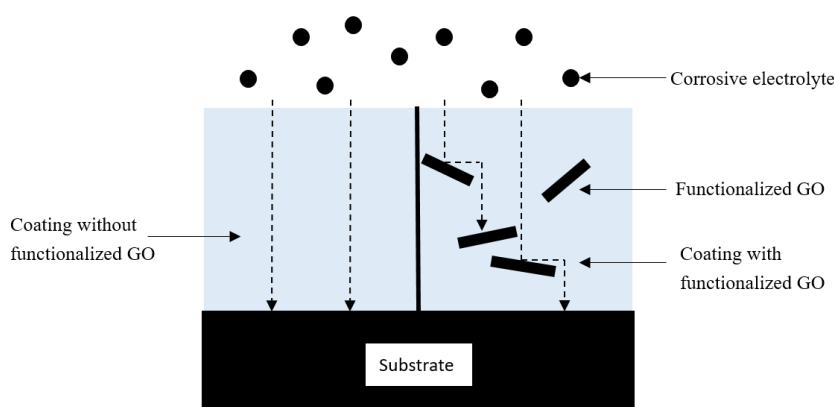

Figure 5. Schematic illustration of coating with and without functionalized GO.

4. CONCLUSION

In conclusion, GO was functionalized by APTES to achieve improved dispersion and was characterized by SEM. The functionalized GO was added into the chemically bonded ceramic coatings to improve the corrosion protection of stainless steel. The results showed that the functionalized GO dispersed well in the ceramic matrix, had a thin layer structure with no cracks, and there was no space between the GO and ceramic matrix. The corrosion performance of the ceramic coatings with functionalized GO was significantly improved when compared with that of the pure ceramic coatings. The enhancement can be mainly attributed to the layer structure as well as the uniform dispersion of the functionalized GO within the ceramic matrix, which effectively increased the tortuosity of diffusion pathways and enhanced the coating impermeability for corrosive electrolytes. In addition, the diffusion pathways were blocked because damaging the bonding between GO and the ceramic matrix consumes a substantial amount of fracture energy.

References

1. E. Colonetti, E. Kammer and A. Junior, *Ceram. Int.*, 40 (2014) 14431.
2. A. Wagh and S. Jeong, *J. Am. Ceram. Soc.*, 86 (2003) 1850.
3. S. Chen, F. Zhang, D. Qin, H. Tao, Y. Yang and Y. Bai, *Int. J. Electrochem. Sci.*, 11 (2016) 3296.
4. H. Colorado, C. Hiel and H. Hahn, *Compos. Pt. A-Appl. Sci. Manuf.*, 42 (2011) 376.
5. D. Bian, Y. Guo and Y. Zhao, *Russ. J. Appl. Chem.*, 89 (2016) 2091.
6. J. Cho, A. Boccaccini and M. Shaffer, *J. Mater. Sci.*, 44 (2009) 1934.
7. Y. Guo, D. Bian and Y. Zhao, *Mater. Res. Express*, 6 (2019) 085021.
8. H. Di, Z. Yu, Y. Ma, Y. Pan, H. Shi, L. Lv, F. Li, C. Wang, T. Long and Y. He, *Polym. Adv. Technol.*, 27 (2016) 915.
9. B. Singh, B. Jena, S. Bhattacharjee and L. Besra, *Surf. Coat. Technol.*, 232 (2013) 475.
10. B. Xue, M. Yu, J. Liu, J. Liu, S. Li and L. Xiong, *J. Alloys Compd.*, 725 (2017) 84.
11. S. Nezamdoust and D. Seifzadeh, *Prog. Org. Coat.*, 109 (2017) 97.
12. F. Chen, Y. Zhang and Y. Zhang, *Int. J. Electrochem. Sci.*, 12 (2017) 6081.
13. Y. Wan, L. Tang, D.Yan, L.Zhao, Y. Li, L. Wu, J. Jiang and G. Lai, *Compos. Sci. Technol.*, 82 (2013) 60.
14. N. Parhizkar, T. Shahrabi and B. Ramezanzadeh, *Corros. Sci.*, 123 (2017) 55.
15. J. Zhao, X. Xie and C. Zhang, *Corros Sci.*, 114 (2017) 146.
16. B. Ramezanzadeh, E. Ghasemi, M. Mahdavian, E. Changizi and M. Moghadam, *Carbon*, 93 (2015) 555.
17. S. Pourhashem, M. Vaezi, A. Rashidi and M. Bagherzadeh, *Corros Sci.*, 115 (2017) 78.
18. Y. Lou, G. Liu, S. Liu, J. Shen and W. Jin, *Appl. Surf. Sci.*, 307 (2014) 631.
19. A. Wagh, S. Grover and S. Jeong, *J. Am. Ceram. Soc.*, 86 (2003) 1845.
20. D. Bian and Y. Zhao, *J. Sol-Gel Sci. Technol.*, 80 (2016) 30.
21. D. Bian, TV. Aradhyula, Y. Guo and Y. Zhao, *Ceram. Int.*, 43 (2017) 12466.
22. C. Chen, S. Qiu, M. Cui, S. Qin, G. Yan, H. Zhao, L. Wang and Q. Xue, *Carbon*, 114 (2017) 356.